Supplementary Material (ESI) for *PCCP*
This journal is © the Owner Societies 2010
Electronic Supplementary Information

Rules and Trends of Metal Cation Driven Hydride-Transfer Mechanisms in Metal Amidoboranes

Dong Young Kim, Han Myoung Lee, Jongcheol Seo, Seung Koo Shin and Kwang S. Kim*

Department of Chemistry, Pohang University of Science and Technology

Pohang, 790-784 (Republic of Korea)

E-mail*: kim@postech.ac.kr

Contents

H_2-loss pathways from dimeric $M(NH_2BH_3)$ (Figure 1d, e).

H_2 is released by as $H^{\delta-}$ atom transfer from a boron atom to a $H^{\delta+}$ atom bonded to a nitrogen atom due to an alkali or alkaline-earth metal cation with/without oligomerization, denoted as the **O**/**D**-pathway. In the **O**/**D**-pathway, the metal hydride *M*–H in $\mathbf{2_M}$ is formed in the first reaction step through $\mathbf{T1_M}$ (1, 2).

$$([M^{I}]^{+}[NH_2BH_3]^{-})_2 \rightarrow NH_2BH_2 + H\text{–}M^{I} + [M^{I}]^{+}[NH_2BH_3]^{-} \quad (1)$$

$$[M^{II}]^{2+}([NH_2BH_3]^{-})_2 \rightarrow NH_2BH_2 + [H\text{–}M^{II}]^{+}[NH_2BH_3]^{-} \quad (2)$$

In the **O**-pathway, the intermolecular N–B bond in $\mathbf{2^O}$ forms through $\mathbf{T2^O}$ (3, 4).

$$NH_2BH_2 + H\text{–}M^{I} + [M^{I}]^{+}[NH_2BH_3]^{-} \rightarrow [M^{I}]^{+}[NH_2BH_2NH_2BH_3]^{-} + H\text{–}M^{I} \quad (3)$$

$$NH_2BH_2 + [H\text{–}M^{II}]^{+}[NH_2BH_3]^{-} \rightarrow [H\text{–}M^{II}]^{+}[NH_2BH_2NH_2BH_3]^{-} \quad (4)$$

Then, first H_2 is released by the ionic recombination of $H^{\delta-}$ with $H^{\delta+}$ through $\mathbf{T2^O_H}$ forming $\mathbf{3^O}$ (5, 6).

$$[M^{I}]^{+}[NH_2BH_2NH_2BH_3]^{-} + H\text{–}M^{I} \rightarrow [M^{I}]^{+}[M^{I}]^{+}[NH_2BH_2NHBH_3]^{2-} + H_2 \quad (5)$$

$$[H\text{–}M^{II}]^{+}[NH_2BH_2NH_2BH_3]^{-} \rightarrow [M^{II}]^{2+}[NH_2BH_2NHBH_3]^{2-} + H_2 \quad (6)$$

Second H_2 also occurs by the formation of *M*–H, $\mathbf{T3^O_M} \rightarrow \mathbf{4^O_M}$ (7, 8), followed by the ionic reaction of the $M\text{–}H^{\delta-}\cdots H^{\delta+}\text{–}N$ dihydrogen bond, $\mathbf{T4^O_H} \rightarrow \mathbf{5^O}$ (9, 10).

$$[M^{I}]^{+}[M^{I}]^{+}[NH_2BH_2NHBH_3]^{2-} \rightarrow H\text{–}\ M^{I} + [M^{I}]^{+}[NH_2BHNHBH_3]^{-} \quad (7)$$

$$[M^{II}]^{2+}[NH_2BH_2NHBH_3]^{2-} \rightarrow [H\text{–}M^{II}]^{+}[NH_2BHNHBH_3]^{-} \quad (8)$$

$$H\text{–}\ M^{I} + [M^{I}]^{+}[NH_2BHNHBH_3]^{-} \rightarrow [M^{I}]^{+}[M^{I}]^{+}[NHBHNHBH_3]^{2-} + H_2 \quad (9)$$

$$[H\text{–}M^{II}]^{+}[NH_2BHNHBH_3]^{-} \rightarrow [M^{II}]^{2+}[NHBHNHBH_3]^{2-} + H_2 \quad (10)$$

In the **D**-pathway, two molar equivalents of H_2 release without oligomerization by the redox reaction of $H^{\delta-}$ and $H^{\delta+}$ in $\mathbf{T2_H} \rightarrow \mathbf{3}$ (11, 12), by the formation of *M*–H in $\mathbf{T3_M} \rightarrow \mathbf{4_M}$ (13, 14), and by the redox reaction of $H^{\delta-}$ and $H^{\delta+}$ in $\mathbf{T4_H} \rightarrow \mathbf{5}$ (15, 16).

$$NH_2BH_2 + H\text{–}M^{I} + [M^{I}]^{+}[NH_2BH_3]^{-} \rightarrow [NHBH_2]^{-}[M^{I}]^{+} + [M^{I}]^{+}[NH_2BH_3]^{-} + H_2 \quad (11)$$

$$NH_2BH_2 + [H\text{–}M^{II}]^{+}[NH_2BH_3]^{-} \rightarrow [NHBH_2]^{-}[M^{II}]^{2+}[NH_2BH_3]^{-} + H_2 \quad (12)$$

$$[NHBH_2]^{-}[M^{I}]^{+} + [M^{I}]^{+}[NH_2BH_3]^{-} \rightarrow [NHBH_2]^{-}[M^{I}]^{+} + NH_2BH_2 + H\text{–}M^{I} \quad (13)$$

$$[NHBH_2]^{-}[M^{II}]^{2+}[NH_2BH_3]^{-} \rightarrow [NHBH_2]^{-}[H\text{–}M^{II}]^{+} + NH_2BH_2 \quad (14)$$

$$[NHBH_2]^{-}[M^{I}]^{+} + NH_2BH_2 + H\text{–}M^{I} \rightarrow ([NHBH_2]^{-}[M^{I}]^{+})_2 + H_2 \quad (15)$$

$$[NHBH_2]^{-}[H\text{–}M^{II}]^{+} + NH_2BH_2 \rightarrow ([NHBH_2]^{-})_2[M^{II}]^{2+} + H_2 \quad (16)$$

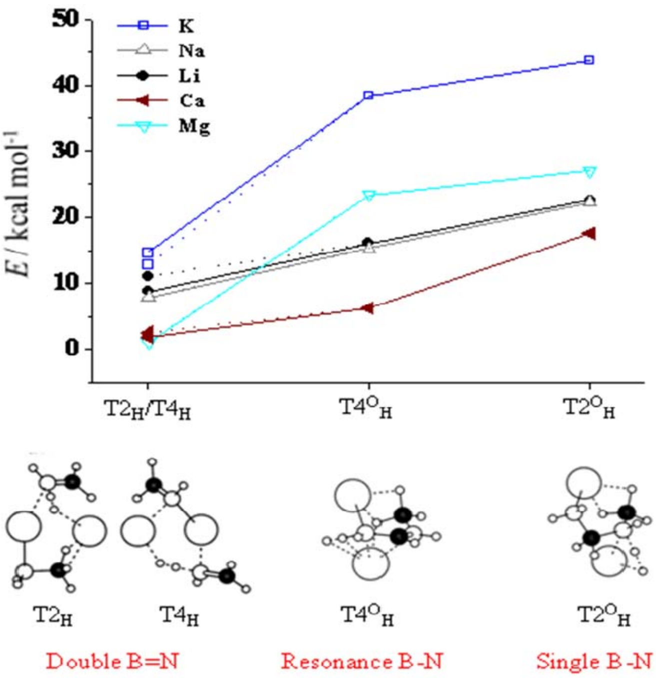

Fig**. S1** Systematic increase of the activation energies in the H-steps. Among the H-steps, either $\mathbf{T2_H}$ or $\mathbf{T4_H}$ leads to the lowest activation barriers, while $\mathbf{T2^O_H}$ leads to the highest barrier.

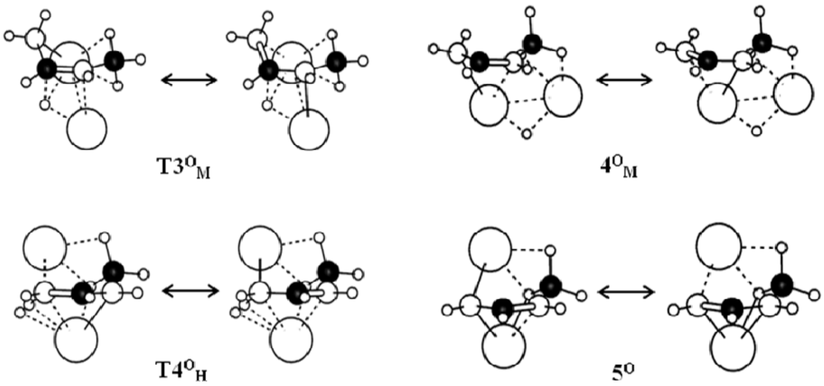

Fig**. S2** Resonance (*M*–N–B=N···*M* ↔ *M*···N=B–N–*M*) hybrid bonds in $\mathbf{T3^{O}_{M}}$, $\mathbf{4^{O}_{M}}$, $\mathbf{T4^{O}_{H}}$ and $\mathbf{5^{O}}$.

Kinetic scheme of the O/D-pathway.

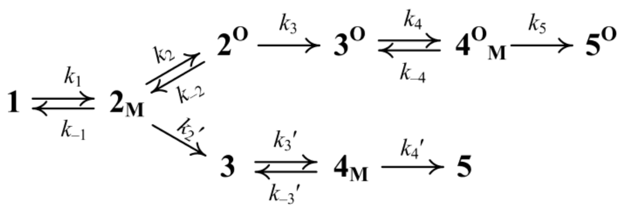

Applying the steady-state approximation, the rate constants are expressed as follows:

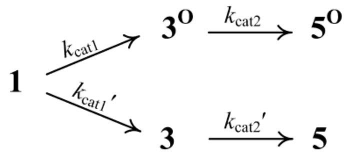

$$k_{cat1} = \frac{k_1 k_2 k_3}{k_C}$$

$$k_{cat2} = \frac{k_4 k_5}{k_{-4} + k_5}$$

$$k_{cat1}{}' = \frac{k_1 k_2{}' (k_{-2} + k_3)}{k_C}$$

$$k_{cat2}{}' = \frac{k_3{}' k_4{}'}{k_{-3}{}' + k_4{}'}$$

$$k_C = (k_{-2} + k_3)(k_{-1} + k_2 + k_2{}') - (k_2 k_{-2})$$

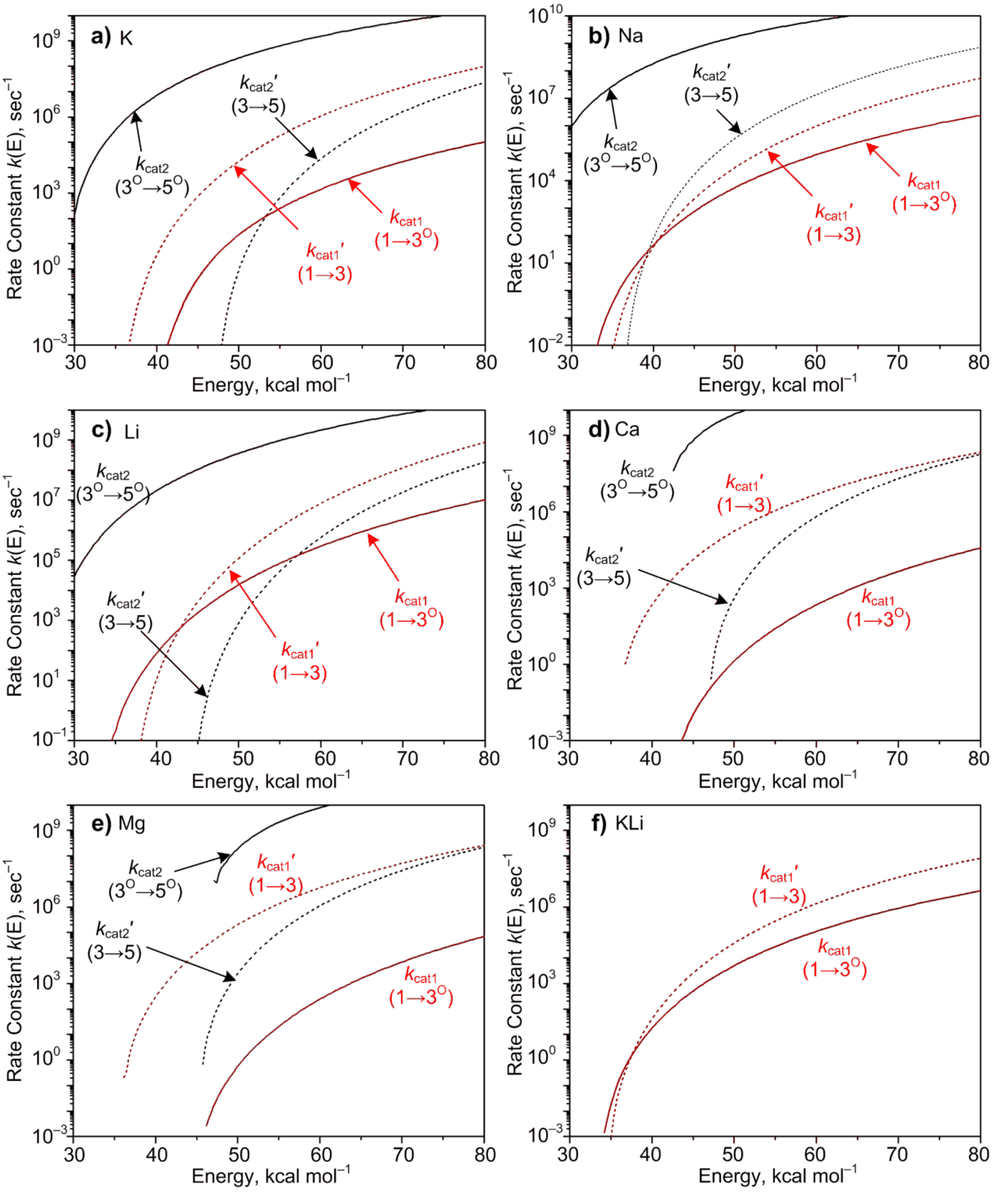

Fig. S3 Microcanonical rate-energy curve at 0 K for the H_2 release of a) $(K^+[NH_2BH_3]^-)_2$, b) $(Na^+[NH_2BH_3]^-)_2$, c) $(Li^+[NH_2BH_3]^-)_2$, d) $Ca^{2+}([NH_2BH_3]^-)_2$, e) $Mg^{2+}([NH_2BH_3]^-)_2$, and f) $K^+Li^+([NH_2BH_3]^-)_2$.

Thermal rate constants of $k_{cat1}/k_{cat1}'/k_{cat2}'$ (in s^{-1}).

Table S1 Rate constants of $k_{cat1}/k_{cat1}'/k_{cat2}'$ (in s^{-1}) at 100–1000 K of the H_2-release reaction in $(K^+[NH_2BH_3]^-)_2$.

T(K)	k_{cat1}	k_{cat1}'	k_{cat2}'
100	1.55×10^{-75}	3.53×10^{-67}	1.20×10^{-64}
200	4.00×10^{-32}	2.82×10^{-27}	3.29×10^{-26}
300	1.41×10^{-17}	6.86×10^{-14}	2.57×10^{-13}
400	2.35×10^{-10}	3.76×10^{-7}	7.98×10^{-7}
500	4.33×10^{-6}	4.41×10^{-3}	6.69×10^{-3}
600	2.69×10^{-3}	2.36×10^{0}	2.87×10^{0}
700	2.49×10^{-1}	2.14×10^{2}	2.23×10^{2}
800	7.07×10^{0}	6.24×10^{3}	5.90×10^{3}
900	8.85×10^{1}	8.13×10^{4}	7.39×10^{4}
1000	5.92×10^{2}	5.61×10^{5}	5.26×10^{5}

Table S2 Rate constants of $k_{cat1}/k_{cat1}'/k_{cat2}'$ (in s^{-1}) at 100–1000 K of the H_2-release reaction in $(Na^+[NH_2BH_3]^-)_2$.

T(K)	k_{cat1}	k_{cat1}'	k_{cat2}'
100	2.62×10^{-59}	2.68×10^{-63}	2.43×10^{-61}
200	3.40×10^{-24}	1.17×10^{-25}	2.75×10^{-24}
300	1.43×10^{-12}	4.94×10^{-13}	7.95×10^{-12}
400	8.80×10^{-7}	1.11×10^{-6}	1.47×10^{-5}
500	2.59×10^{-3}	7.58×10^{-3}	8.63×10^{-2}
600	5.31×10^{-1}	2.80×10^{0}	2.83×10^{1}
700	2.39×10^{1}	1.94×10^{2}	1.77×10^{3}
800	4.14×10^{2}	4.67×10^{3}	3.92×10^{4}
900	3.72×10^{3}	5.33×10^{4}	4.28×10^{5}
1000	2.01×10^{4}	3.39×10^{5}	2.76×10^{6}

Table S3 Rate constants of $k_{cat1}/k_{cat1}'/k_{cat2}'$ (in s^{-1}) at 100–1000 K of the H_2-release reaction in $(Li^+[NH_2BH_3]^-)_2$.

T(K)	k_{cat1}	k_{cat1}'	k_{cat2}'
100	6.65×10^{-63}	5.68×10^{-70}	4.04×10^{-67}
200	1.11×10^{-25}	2.85×10^{-28}	3.19×10^{-27}
300	2.71×10^{-13}	3.33×10^{-14}	8.72×10^{-14}
400	4.15×10^{-7}	4.13×10^{-7}	5.20×10^{-7}
500	2.14×10^{-3}	7.98×10^{-3}	6.47×10^{-3}
600	6.43×10^{-1}	5.99×10^{0}	3.62×10^{0}
700	3.83×10^{1}	6.95×10^{2}	3.42×10^{2}
800	8.23×10^{2}	2.46×10^{4}	1.05×10^{4}
900	8.77×10^{3}	3.73×10^{5}	1.49×10^{5}
1000	5.44×10^{4}	2.93×10^{6}	1.18×10^{6}

Table S4 Rate constants of $k_{cat1}/k_{cat1}'/k_{cat2}'$ (in s^{-1}) at 100–1000 K of the H_2-release reaction in $Ca^{2+}([NH_2BH_3]^-)_2$.

T(K)	k_{cat1}	k_{cat1}'	k_{cat2}'
100	1.67×10^{-83}	3.85×10^{-67}	4.35×10^{-65}
200	1.17×10^{-36}	3.01×10^{-27}	2.40×10^{-26}

300	4.96×10^{-21}	6.70×10^{-14}	2.59×10^{-13}
400	3.40×10^{-13}	3.41×10^{-7}	9.38×10^{-7}
500	1.78×10^{-8}	3.76×10^{-3}	8.44×10^{-3}
600	2.57×10^{-5}	1.90×10^{0}	3.75×10^{0}
700	4.70×10^{-3}	1.65×10^{2}	2.97×10^{2}
800	2.33×10^{-1}	4.70×10^{3}	7.99×10^{3}
900	4.61×10^{0}	6.25×10^{4}	1.04×10^{5}
1000	4.51×10^{1}	4.69×10^{5}	7.88×10^{5}

Table S5 Rate constants of $k_{cat1}/k_{cat1}'/k_{cat2}'$ (in s^{-1}) at 100–1000 K of the H_2-release reaction in $Mg^{2+}([NH_2BH_3]^-)_2$.

T(K)	$\boldsymbol{k_{cat1}}$	$\boldsymbol{k_{cat1}}'$	$\boldsymbol{k_{cat2}}'$
100	5.19×10^{-89}	3.01×10^{-67}	6.05×10^{-67}
200	8.05×10^{-39}	2.22×10^{-27}	2.94×10^{-27}
300	3.90×10^{-22}	5.46×10^{-14}	6.35×10^{-14}
400	8.36×10^{-14}	2.95×10^{-7}	3.25×10^{-7}
500	8.33×10^{-9}	3.37×10^{-3}	3.62×10^{-3}
600	1.80×10^{-5}	1.75×10^{0}	1.86×10^{0}
700	4.38×10^{-3}	1.56×10^{2}	1.64×10^{2}
800	2.65×10^{-1}	4.56×10^{3}	4.80×10^{3}
900	6.02×10^{0}	6.22×10^{4}	6.65×10^{4}
1000	6.47×10^{1}	4.77×10^{5}	5.33×10^{5}

Table S6 Rate constants of k_{cat1}/k_{cat1}' (in s^{-1}) at 100–1000 K of the H_2-release reaction in $(Li^+[NH_2BH_2CH_3]^-)_2$ and $K^+Li^+([NH_2BH_3]^-)_2$.

	$(Li^+[NH_2BH_2CH_3]^-)_2$	$K^+Li^+([NH_2BH_3]^-)_2$	
T(K)	$\boldsymbol{k_{cat1}}$	$\boldsymbol{k_{cat1}}$	$\boldsymbol{k_{cat1}}'$
100	7.99×10^{-63}	3.56×10^{-63}	1.43×10^{-64}
200	1.73×10^{-24}	6.63×10^{-26}	3.47×10^{-26}
300	1.50×10^{-11}	1.58×10^{-13}	2.65×10^{-13}
400	5.08×10^{-5}	2.35×10^{-7}	8.06×10^{-7}
500	4.50×10^{-1}	1.18×10^{-3}	6.60×10^{-3}
600	2.01×10^{2}	3.48×10^{-1}	2.77×10^{0}
700	1.58×10^{4}	2.03×10^{1}	2.12×10^{2}
800	3.80×10^{5}	4.31×10^{2}	5.49×10^{3}
900	3.60×10^{6}	4.50×10^{3}	6.65×10^{4}
1000	1.60×10^{7}	2.72×10^{4}	4.43×10^{5}

Relative energies along the reaction pathways.

Table S7 MP2/6-311++G** relative energies (*ΔE*) and ZPE-corrected energies (*ΔE₀*) for $(K^+/Na^+/Li^+[NH_2BH_3]^-)_2$ and $Ca^{2+}/Mg^{2+}([NH_2BH_3]^-)_2$ along the **O**-pathway.

		1	**T1$_M$**	**2$_M$**	**T2^O**	**2^O**	**T2^O_H**	**3^O**	**T3^O_M**	**4^O_M**	**T4^O_H**	**5^O**
K	*ΔE*	0.00	39.36	33.92	41.83	17.96	36.46	15.81	38.56	22.45	31.57	20.89
	ΔE$_0$	0.00	36.14	30.90	39.12	17.35	34.88	9.30	29.73	14.38	20.62	8.49
Na	*ΔE*	0.00	32.76	29.13	34.13	9.99	35.73	18.33	35.41	17.32	35.21	21.93
	ΔE$_0$	0.00	30.00	26.31	31.84	10.02	32.25	12.01	26.82	9.57	24.79	9.59
Li	*ΔE*	0.00	31.08	29.50	32.34	11.91	37.87	12.17	30.51	20.27	39.39	19.88
	ΔE$_0$	0.00	27.85	26.48	29.95	11.42	34.00	5.94	21.83	11.92	28.00	7.06
Ca	*ΔE*	0.00	39.27	36.29	39.25	16.46	46.38	39.77	45.32	27.25	52.87	42.48
	ΔE$_0$	0.00	35.72	33.36	36.49	15.90	42.92	33.38	37.23	18.92	42.34	29.54
Mg	*ΔE*	0.00	26.21	26.19	27.00	2.15	49.46	43.49	47.49	16.92	58.28	45.97
	ΔE$_0$	0.00	23.07	23.35	24.76	2.18	45.95	36.43	38.90	8.67	47.12	31.85

Table S8 MP2/6-311++G** relative energies (*ΔE*) and ZPE-corrected energies (*ΔE₀*) for $(K^+/Na^+/Li^+[NH_2BH_3]^-)_2$ and $Ca^{2+}/Mg^{2+}([NH_2BH_3]^-)_2$ along the **D**-pathway.

		T2$_H$	**3**	**T3$_M$**	**4$_M$**	**T4$_H$**	**5**
K	*ΔE*	39.22	20.20	58.08	53.48	57.98	39.00
	ΔE$_0$	33.46	12.77	47.64	42.99	44.73	23.84
Na	*ΔE*	39.67	18.11	51.37	46.61	57.47	35.31
	ΔE$_0$	34.21	10.77	41.15	36.52	44.28	20.68
Li	*ΔE*	44.02	16.39	47.76	46.35	58.58	32.21
	ΔE$_0$	37.55	8.71	37.20	36.04	44.81	17.26
Ca	*ΔE*	39.86	19.51	58.13	55.99	59.36	39.21
	ΔE$_0$	34.48	11.94	47.01	45.37	46.37	24.02
Mg	*ΔE*	41.41	17.27	42.10	41.55	58.46	34.87
	ΔE$_0$	36.14	9.60	31.54	30.99	45.57	19.55

Table S9 MP2/6-311++G** relative energies (*ΔE*) and ZPE corrected energies (*ΔE₀*) for $K^+Li^+([NH_2BH_3]^-)_2$ along the **O**/**D**-pathway.

	1	**T1$_M$**	**2$_M$**	**T2^O**	**2^O**	**T2^O_H**	**3^O**	**T2$_H$**	**3**
ΔE	0.00	34.32	31.04	35.10	14.51	37.92	14.45	40.25	17.11
ΔE$_0$	0.00	31.42	28.13	32.86	14.24	34.10	8.32	34.83	9.81

Table S10 MP2/6-311++G** relative energies (*ΔE*) and ZPE corrected energies (*ΔE₀*) for $(Li^+[NH_2BH_2CH_3]^-)_2$ along the **D**-pathway.

	1	**T1$_M$**	**2$_M$**	**T2$_H$**	**3**
ΔE	0.00	25.30	24.32	40.88	13.30
ΔE$_0$	0.00	22.33	21.20	34.40	5.65